

## Supplementary materials

### Dynamic FeO<sub>x</sub>/FeWO<sub>x</sub> nanocomposite memristor for neuromorphic and reservoir computing

Muhammad Ismail<sup>a</sup>, Maria Rasheed<sup>b</sup>, Yongjin Park<sup>a</sup>, Jungwoo Lee<sup>a</sup>, Chandreswar Mahata<sup>a</sup> and Sungjun Kim<sup>\*a</sup>

<sup>a</sup> Division of Electronics and Electrical Engineering, Dongguk University, Seoul 04620, South Korea

<sup>b</sup> Department of Advanced Battery Convergence Engineering, Dongguk University, Seoul 04620, Republic of Korea

\* Corresponding author: [sungjun@dongguk.edu](mailto:sungjun@dongguk.edu) (S. Kim)

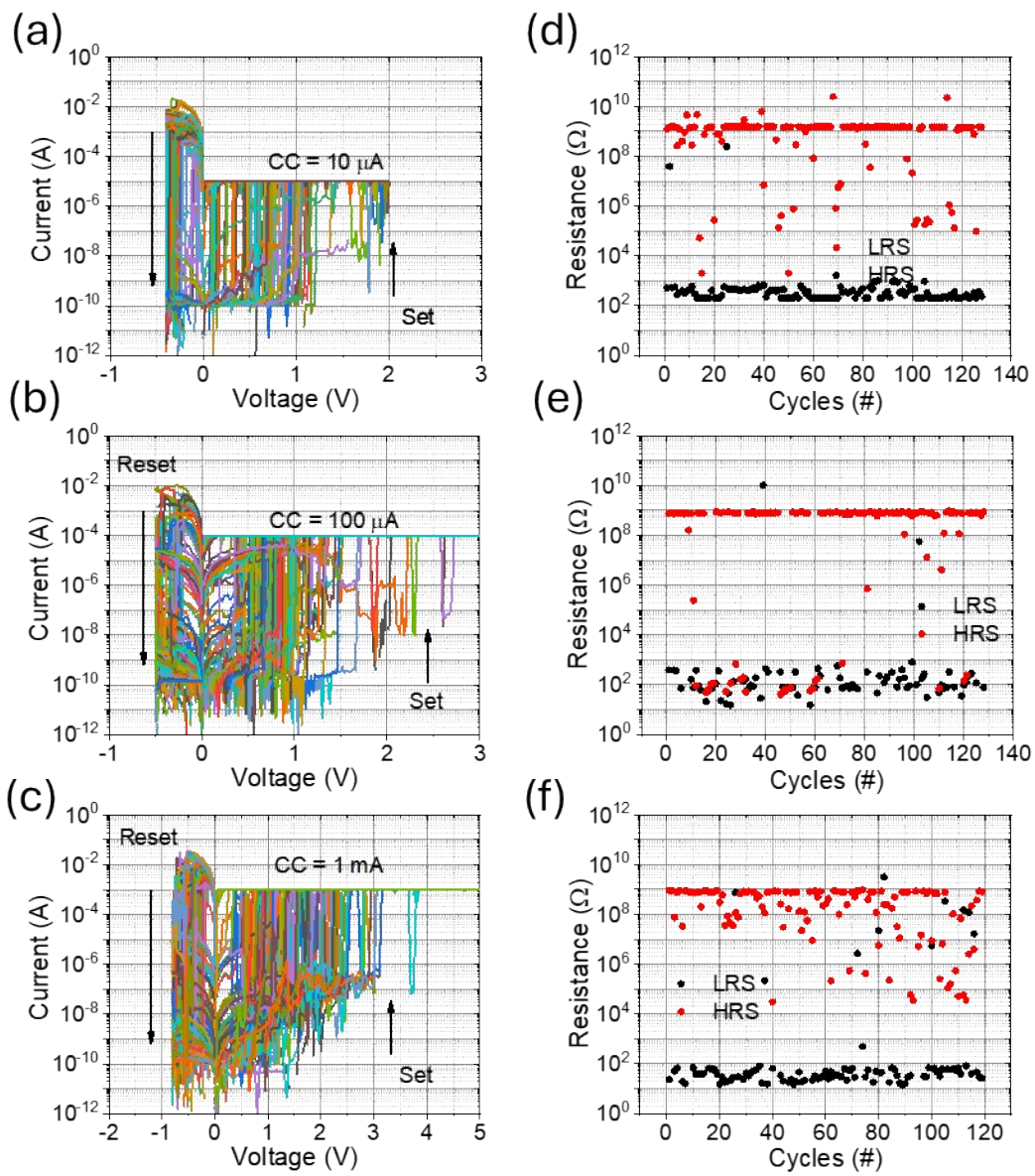


Fig. S1. Digital resistive switching characteristics of Ag/FeWO<sub>x</sub>/Pt memristor under varying current compliance levels of 10  $\mu\text{A}$ , 100  $\mu\text{A}$ , and 1 mA, respectively.

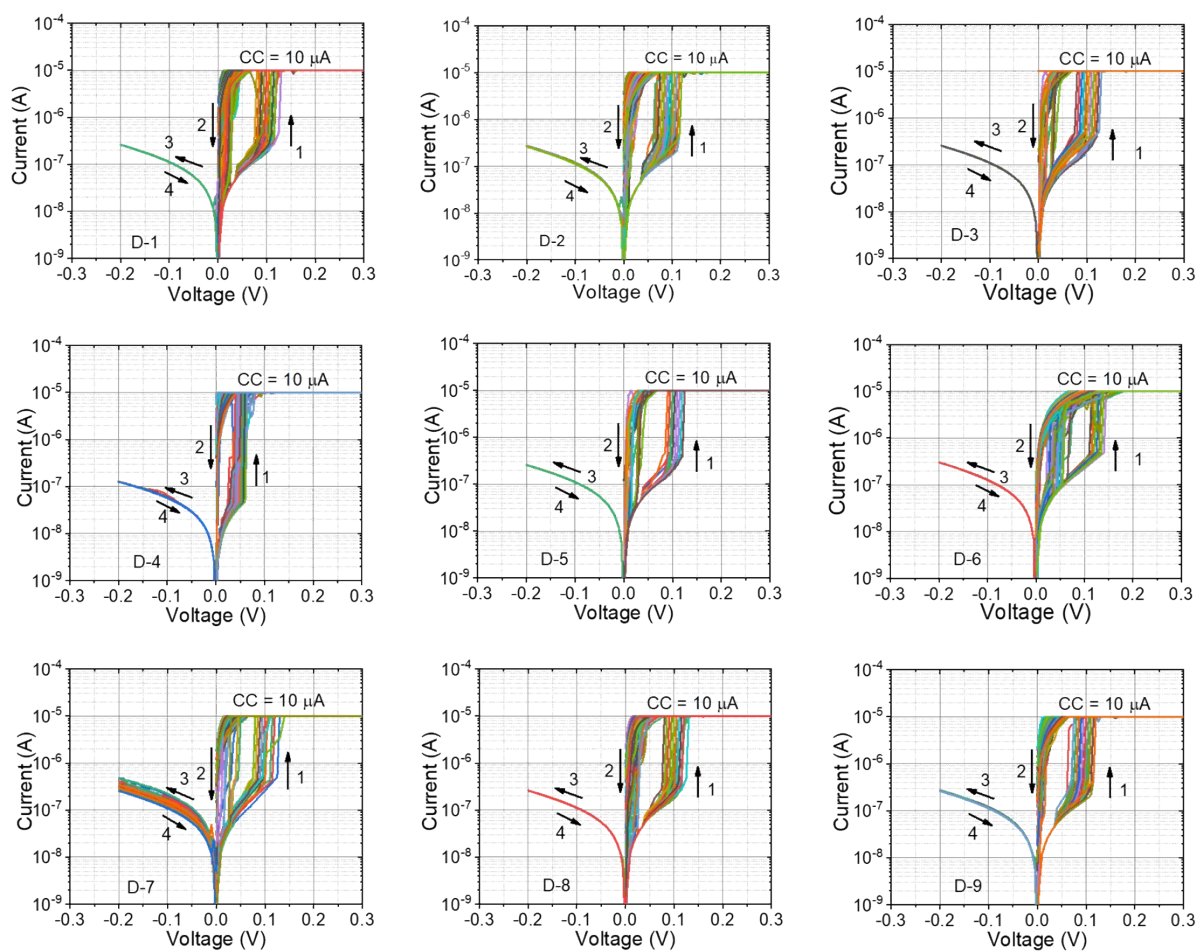


Fig. S2. Device-to-device (D2D) variability and reproducibility. (D1-D9) Demonstration of typical resistive switching behavior for different memory devices of FeOx/FeWOx nanocomposite based memristors. The I-V curves were recorded over 100 cycles during the cyclic test. Arrows and numbers indicate the sweep direction.

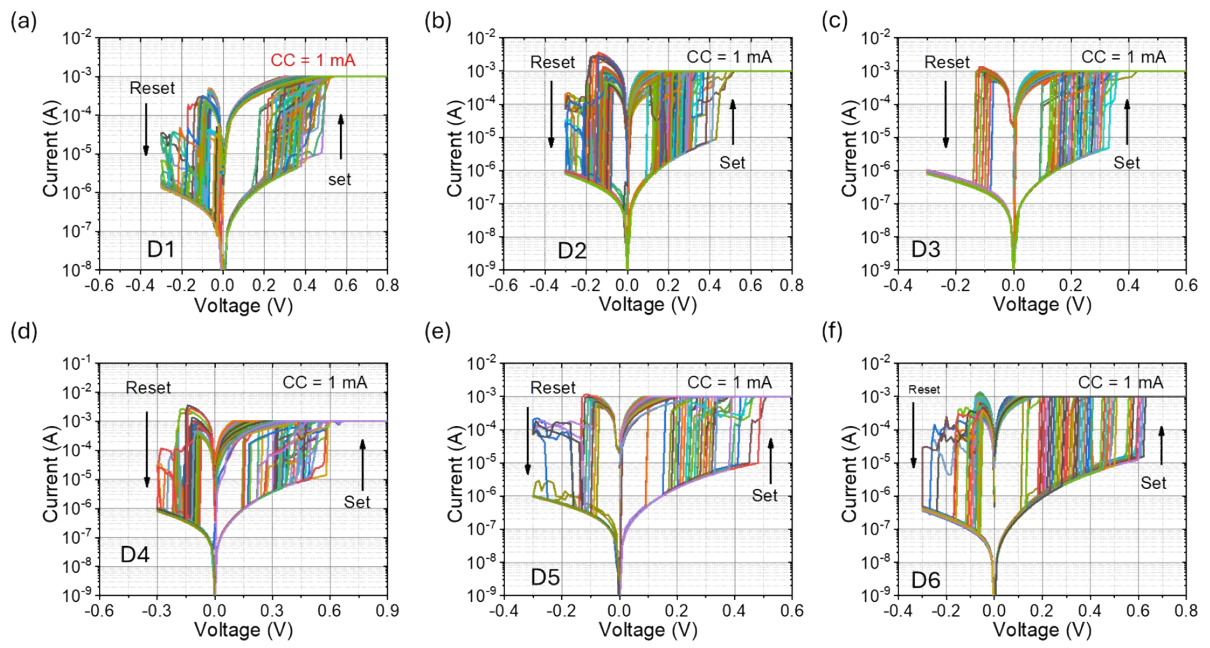


Fig. S3. Device-to-device (D2D) variability and reproducibility of FeOx/FeWOx nanocomposite memristors, showing typical digital resistive switching behavior for six randomly selected devices. The I-V curves were recorded over 100 cycles with a current compliance of 1 mA. Arrows and numbers indicate the sweep direction.

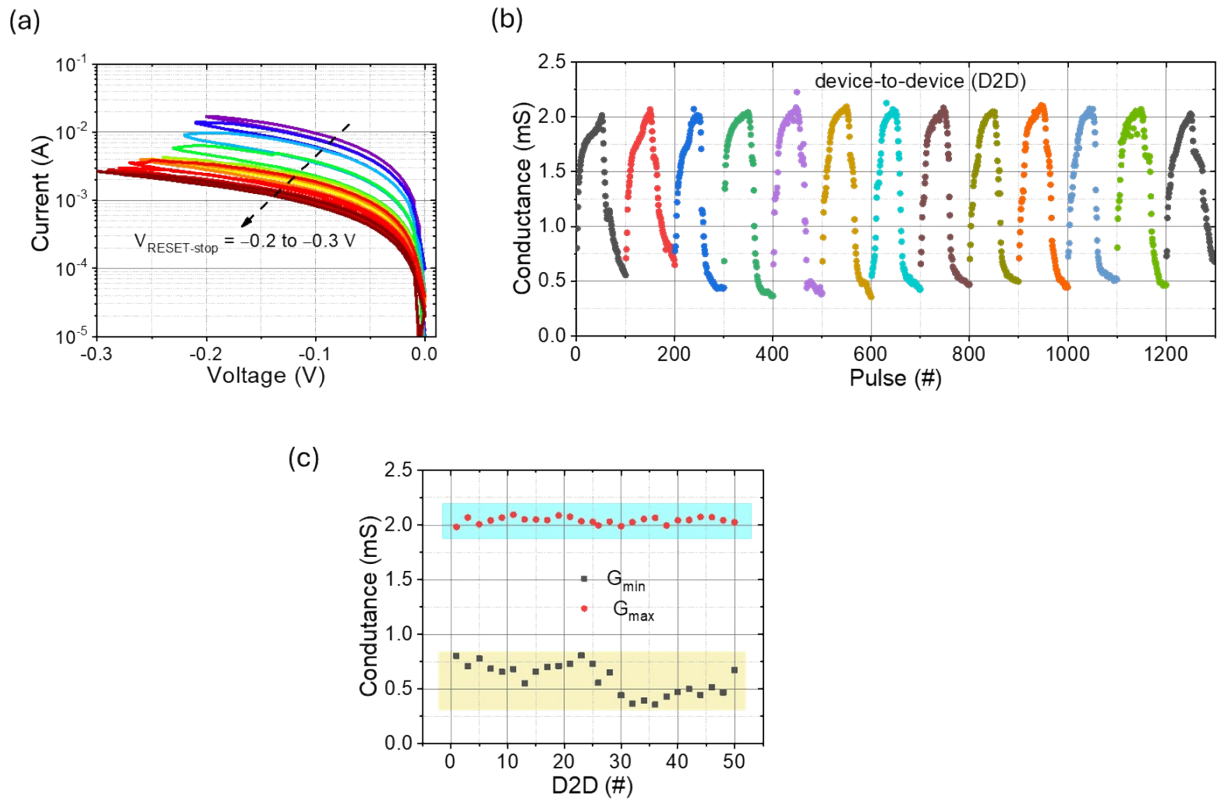


Fig. S4. (a) Continuous regulation of the FeOx/FeWOx nanocomposite memristor device current is achieved by varying the reset-stop voltage from  $-0.2$  V to  $-0.3$  V in  $0.01$  V increments, demonstrating the analog switching behavior. (b) Variability in conductance states among memristor devices during both the potentiation and depression processes, observed across 12 randomly selected devices. (c) Variation in the  $G_{\text{max}}$  and  $G_{\text{min}}$  values during the potentiation and depression processes across 50 devices.

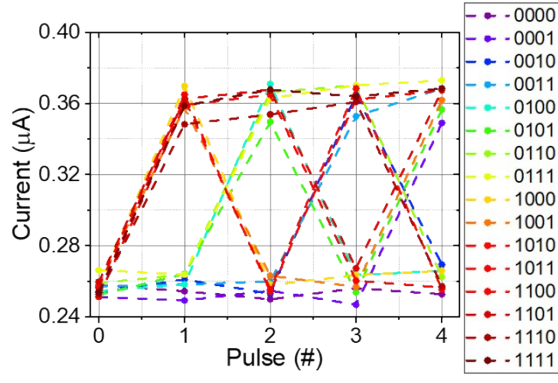
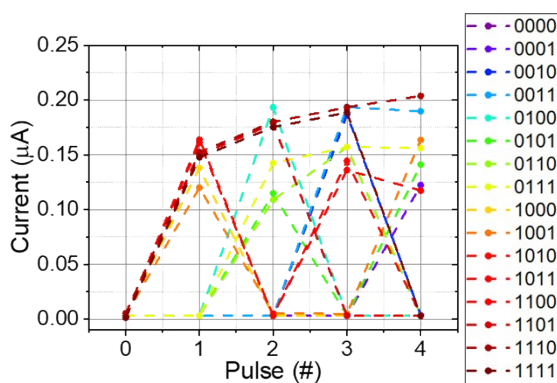
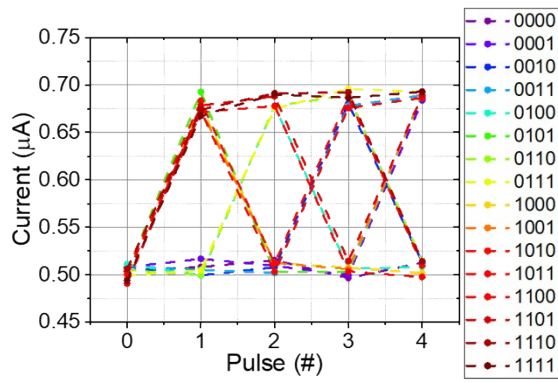
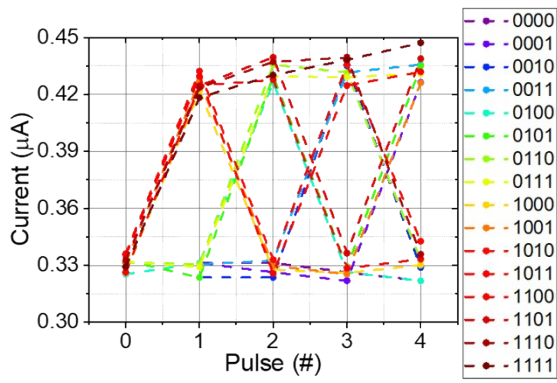


Fig. S5. Device-to-device variability across 16 different states, analyzed by randomly selecting four memory devices of FeOx/FeWOx nanocomposite based memristors, with four bits used as physical reservoir computing.

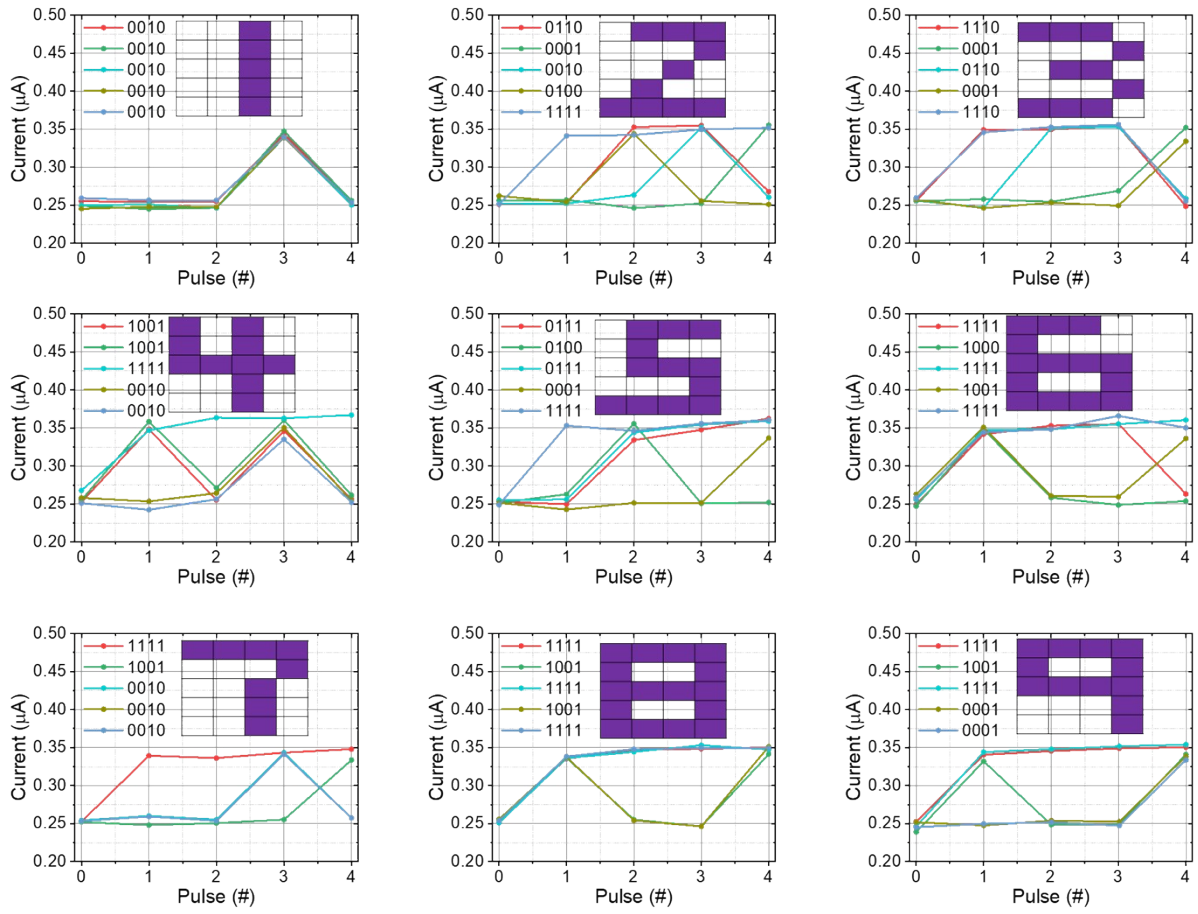


Fig. S6. Reservoir states measured after subjecting the memristors to 9 distinct inputs. The states are represented by the read currents of the 0.3 memristors that constitute the reservoir. Insets show the images labeled 1 through 9 used in this test.

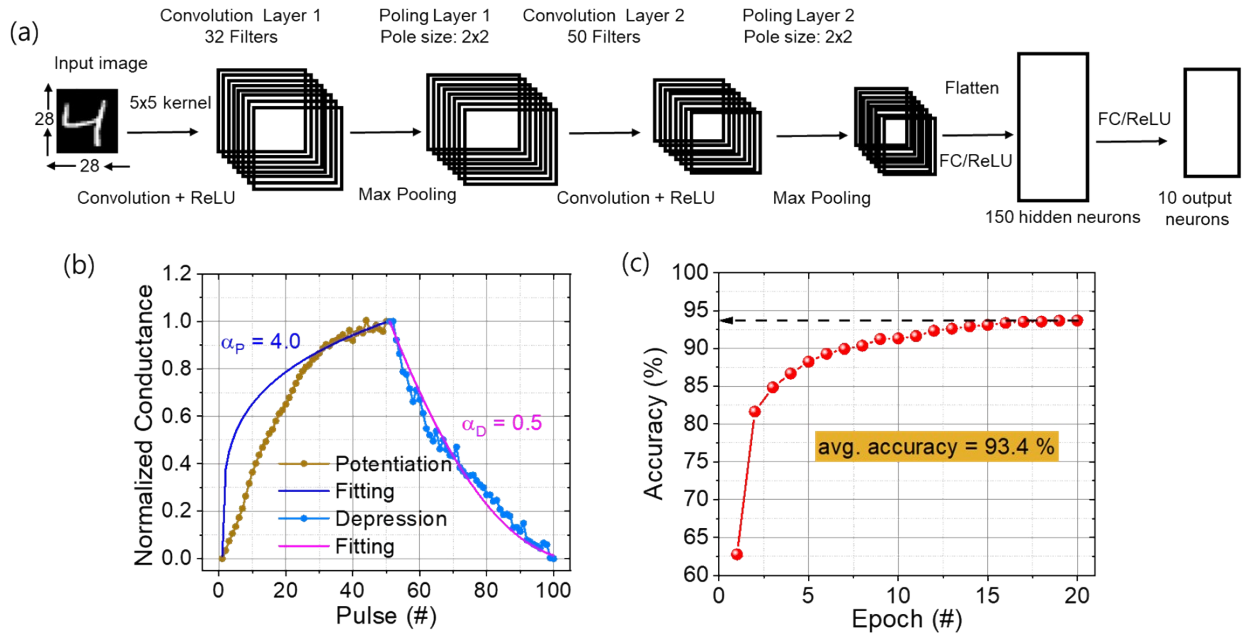
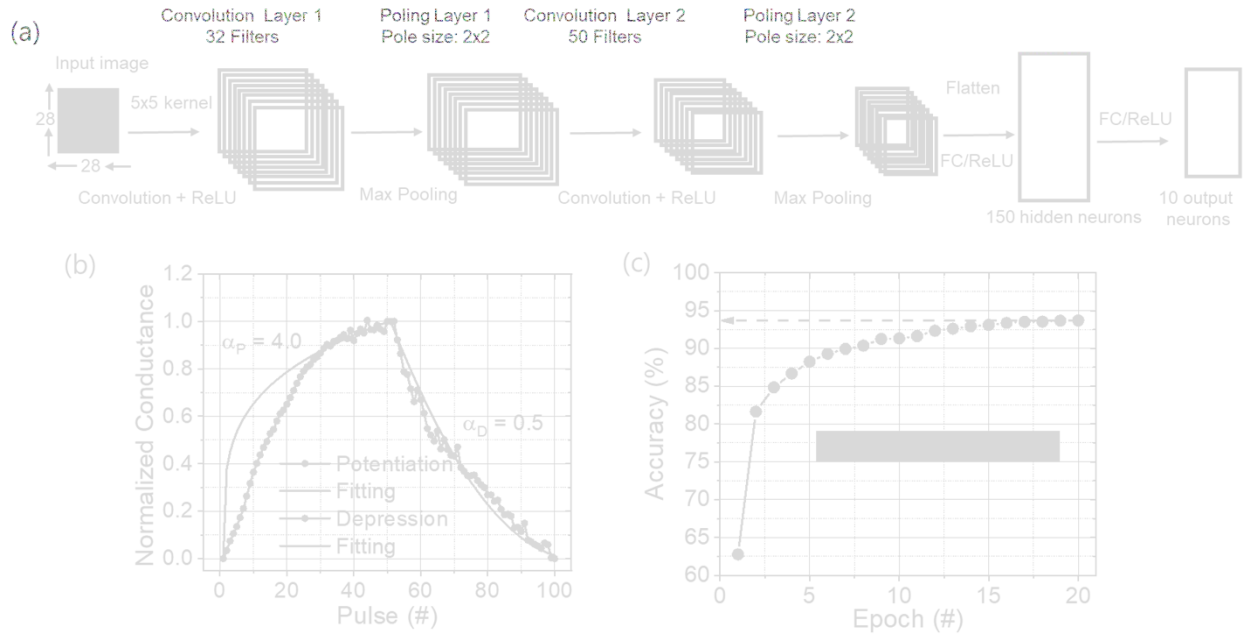


Fig. S7. (a) Schematic diagram of the Convolutional Neural Network (CNN) designed to identify the digit "3". (b) Potentiation and depression data used in the accuracy simulation. (c) Simulated pattern recognition accuracy of the CNN during training, achieving 93.4% accuracy with MNIST database images.



**Fig. S7.** (a) Schematic diagram of the Convolutional Neural Network (CNN) designed to identify the digit “3”. (b) Potentiation and depression data used in the accuracy simulation. (c) Simulated pattern recognition accuracy of the CNN during training, achieving 93.4% accuracy with MNIST database images.

Table 1 compares switching parameters, synaptic plasticity, switching speed, and reservoir computing capabilities between previously published CBRAM bilayer structures and FeO<sub>x</sub>/FeWO<sub>x</sub>-based CBRAM, highlighting the specific advantages associated with FeO<sub>x</sub>/FeWO<sub>x</sub>.

Memristor structure	Compliance Current Dependency	Switching Mode	Retention (s)	DC Endurance (cycles)	Switching Speed	Operating Voltage	Synaptic plasticity	Reservoir computing	Refs.
Cu/TiO <sub>x</sub> /MoS <sub>2</sub> /Pt	Yes	Non-volatile	No	2000	5.7 pJ	1/-1 V	Yes	No	1
Ag/ZnO/GO/Cu	Yes	Non-volatile	10 <sup>4</sup>	3000	No	3.8/-3.1 V	No	No	2
Pt-Ag/SiO <sub>2</sub> :Ag/p++-Si	Yes	Non-volatile	10 <sup>4</sup>	No	No	2.5/-3.5 V	Yes	No	3
Ag/HfO <sub>x</sub> :N/Pt	Yes	Volatile	No	100	1.5 ms	0.2 V	No	No	4
Ag/a-TiO <sub>2</sub> /a-TiO <sub>2</sub> /p-Si	Yes	Non-volatile	No	No	No	2.5/-3 V	Yes	No	5
Cu/TaO <sub>x</sub> /CNT	Yes	Volatile/Non-volatile	10 <sup>4</sup>	500	No	2.3/-0.9 V	No	No	6
Ag/FeO <sub>x</sub> /FeWO <sub>x</sub> /Pt	Yes	Volatile/Non-volatile	10 <sup>4</sup>	500	0.1fJ	~ 0.2 V	Yes	Yes	This work

FeO<sub>x</sub>/FeWO<sub>x</sub>-based CBRAM stands out due to its high endurance and stable retention, making it suitable for applications that demand reliability and consistent performance. Although FeO<sub>x</sub>/FeWO<sub>x</sub> offers these advantages, it requires a higher forming voltage and may introduce integration complexities, potentially impacting large-scale fabrication. However, the FeO<sub>x</sub>/FeWO<sub>x</sub> bilayer’s ability to balance volatile and non-volatile switching modes while ensuring stable, low-power operation is particularly valuable for applications needing tunable switching behaviors.

In the comparison above, each study exhibits distinct trade-offs in terms of endurance, retention, switching speed, and compliance current dependency. Evaluating these findings within specific application requirements is essential to balancing the strengths and limitations of each bilayer structure to optimize device performance.

#### References.

- 1 S. Ginnaram, S. Maikap, Journal of Physics and Chemistry of Solids 2021,151, 109901.
- 2 R. Tian, L. Li, K. Yang, Z. Yang, H. Wang, P. Pan, J. He, J. Zhao, B. Zhou, Vacuum 2023, 207, 111625.
- 3 D. Li, N. Ilyas, C. Li, X. Jiang, Y. Jiang, W. Li, J. Phys. D: Appl. Phys.2020, 53, 175102.
- 4 J.-H. Park, S.-H. Kim, S.-G. Kim, K.Heo, H.-Y. Yu, ACS Appl. Mater. Interfaces 2019, 11, 9182–9189.
- 5 S. H. Choi, S.-O. Park, S. Seo, S. Choi,Sci. Adv.2022, 8, eabj7866.
- 6 J. Kim, J. H. Choi, S. Kim, C. Choi, S. Kim, Carbon 2023, 215, 118438.